CZECH TECHNICAL UNIVERSITY IN PRAGUE

FACULTY OF MECHANICAL ENGINEERING

DOCTORAL THESIS STATEMENT

ČESKÉ VYSOKÉ UČENÍ TECHNICKÉ V PRAZE

FAKULTA STROJNÍ

ÚSTAV MECHANIKY, BIOMECHANIKY A MECHATRONIKY

TEZE DISERTAČNÍ PRÁCE

Mechanical Properties of Perivascular Adipose Tissue and its Effect on Biomechanics of Abdominal Aorta

Tereza Voňavková

Doktorský studijní program: Strojní inženýrství

Studijní obor: Biomechanika

Školitel: Doc. Ing. Lukáš Horný, Ph.D.

Teze disertace k získání akademického titulu "doktor", ve zkratce "Ph.D."

Praha Červen 2020

Disertační práce byla vypracována v prezenční a následně v kombinované formě doktorského studia na Ústavu mechaniky, biomechaniky a mechatroniky, Fakulty strojní ČVUT v Praze.

Disertant: Ing. Tereza Voňavková
Ústav mechaniky, biomechaniky a mechatroniky
Fakulta strojní ČVUT v Praze
Technická 4, Praha 6 166 07

Školitel: Doc. Ing. Lukáš Horný, Ph.D.
Ústav mechaniky, biomechaniky a mechatroniky
Fakulta strojní ČVUT v Praze
Technická 4, Praha 6 166 07

Oponenti:

Teze byly rozeslány dne: .....

Obhajoba disertace se koná dne ..... v …… hod.

v zasedací místnosti č. 17 (v přízemí) Fakulty strojní ČVUT v Praze, Technická 4, Praha 6

před komisí pro obhajobu disertační práce ve studijním oboru Biomechanika.

S disertací je možno se seznámit na oddělení vědy a výzkumu Fakulty strojní ČVUT v Praze, Technická 4, Praha 6.

předseda oborové rady oboru Biomechanika:

prof. RNDr. Matěj Daniel, Ph.D.

Fakulta strojní ČVUT v Praze

Table of content

1. Introduction

Cardiovascular diseases are still the most frequent cause of death in developed countries, regardless of innovations that have appeared in last decades. New treatment approaches cannot be introduced without highly multidisciplinary research that combines knowledge from medical, biological, biochemical, and also engineering sciences. A way how engineering sciences can contribute to the progress in medicine are biomechanical simulations.

Biomechanical simulations can significantly reduce expensive and ethically problematic experiments determining an interaction between diseased tissues and therapeutic instruments. They make possible to predict whether some procedures, for example percutaneous intervention, will be successful or not (Fereidoonnezhad et al., 2017; Holzapfel et al., 2005). Computational simulations can also help to determine the optimal design of stents and prostheses (Kiousis et al, 2007) and to identify conditions leading to aneurysm rupture (Hejčl et al., 2017; Polzer and Gasser, 2015). Such simulations, however, have to be based on reliable data describing geometry, internal structure, mutual bonds, and the constitutive properties of interacting bodies.

Despite significant progress that has been achieved in arterial biomechanics, there are still topics that seem to have been overlooked for a long time. In the author's opinion, one of these is the role of perivascular adipose tissue (PVAT); see Figure 1 for detailed view of the infrarenal abdominal region (the aorta surrounded with adipose tissue). It may have been a widely accepted idea that perivascular tissue provides mechanical support to an artery, but it has led to a clear oversimplification in which one imagines the role of perivascular adipose tissue in the way that it merely fills the space between the external surface of the artery and neighboring organs. The

current anatomical and physiological view of the role of PVAT is, however, quite different.

Similar to the endothelium, PVAT can modulate vascular tone by releasing vasoactive molecules (the adipocyte-derived relaxing factor, NO, prostacyclin, and H_2O_2; Zaborska et al., 2017) which has a direct impact on the mechanical state of the artery. In contrast to the endothelium, PVAT consists of multiple cell types. Besides adipocytes, macrophages, fibroblasts, lymphocytes, and adipocyte progenitor cells are also present in perivascular adipose tissue. The presence of these types of cells suggests the complex endocrine function of PVAT and its contribution to inflammatory processes occurring in the arterial wall (Zaborska et al., 2017; Brown et al., 2014; Králová Lesná et al., 2015). Considering this, one sees that PVAT is not merely a mechanical support mechanism, nor a simple energy-storing tissue, but it is an element with its own complex mechanobiological role that can affect the onset of various cardiovascular diseases (Huang Cao et al., 2017).

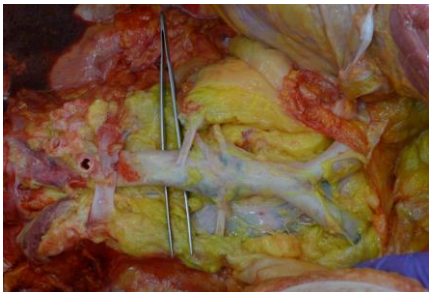

Figure 1. Infrarenal abdominal aorta surrounded by perivascular adipose tissue. Renal arteries stem from the aorta on the left side of the figure, and common iliac arteries continue from the aorta on right part of the figure. The picture from author's personal archive.

Nevertheless, it is not only the biological function of PVAT that seems to be underrated in the scientific literature. Computational simulations describing arterial biomechanics considering the effect of perivascular tissue are also

rare. If the effect of perivascular tissue is considered, it is most frequently reduced to a form of the boundary condition imposed at the external surface of the artery and the most of studies even simplify a situation to a state in which the external pressure is considered to be zero. Thus no force acting between modeled artery and its surroundings is included to the model. This simplification may be adopted when pure tissue mechanics is studied. However, when one wants to study in vivo behavior to obtain predictions suitable for medical or treatment decisions, like in case of risk of aneurysm rupture evaluation, so in this case one should be as close to the reality as it is possible and in the real body, the abdominal aorta is surrounded by adipose tissue.

The approach expressing mechanical interaction between an artery and surrounding tissue by means of external pressure has been adopted by Zhang et al. (2004) and Moireau et al. (2012) who investigated the effect of the surrounding tissue on hemodynamics in the aorta. Hodis and Zamir (2009, 2011) investigated the effect of external tethering of the arterial wall on the dynamics of pressure pulse transmission. Their simulations were based on a 3D linearized viscoelastic model and showed that the surrounding tissue can have an important effect, again accounted for by means of the external boundary condition, on wall stress variation, and pulse wave velocity. Stress and strain variation and pulse velocity were reduced when external support was considered in their simulations (Hodis and Zamir, 2009, 2011).

With regard to elastostatics, Liu et al. (2007) obtained pressure-radius experimental data from swine carotid and femoral arteries in the tethered state and after PVAT excision. They showed that arteries with surrounding tissue sustain lower strains and stresses during inflation than their untethered counterparts, Figure 2. Masson et al. (2011) considered perivascular support in their computational model when estimating the constitutive parameters of human carotid arteries from in vivo data. They used the model of the thick-walled tube for the artery; however, the perivascular tissue was again reduced

only to its mechanical interaction with the wall by nonzero external pressure acting on the artery by means of the mathematical expression for perivascular pressure proposed by Humphrey and Na (2002).

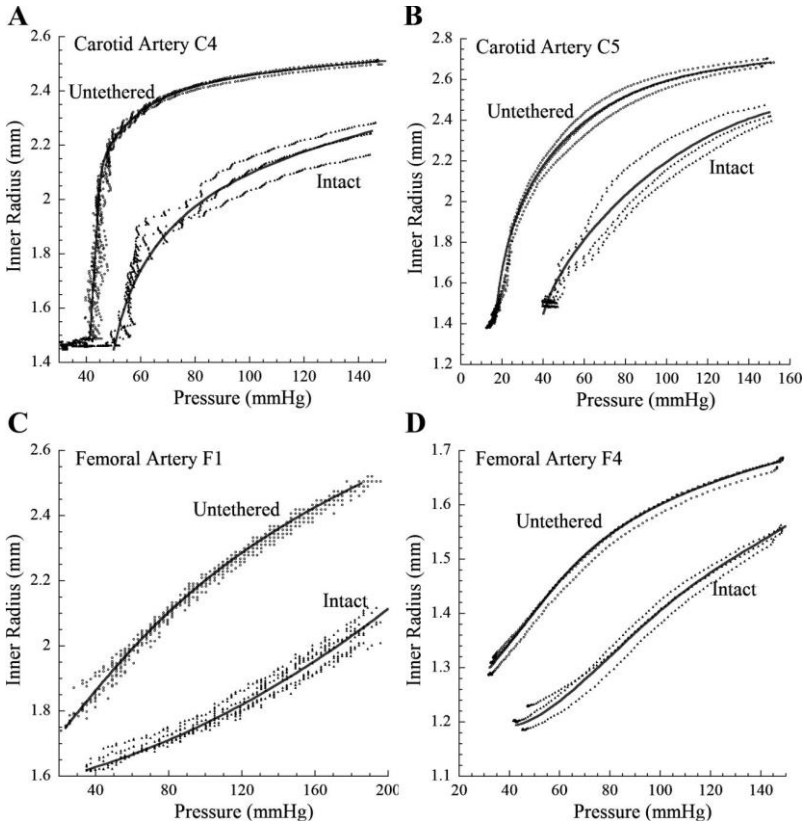

Figure 2. Pressure–radius relationships for swine carotid and femoral arteries obtained experimentally by Liu et al. (2007). Intact arteries contained adipose tissue envelop whereas in case of untethered samples the adipose tissue was dissected. Notice that untethered samples exhibit larger deformations and one also can say that their response shows higher degree of nonlinearity.

It is clear that approach implementing surrounding tissue as the boundary condition has its weak point in a fact that this pressure cannot be measured

directly. To the best of author's knowledge, there are only two works where experiments focused on determining this pressure have been carried out. It is above mentioned study by Liu et al. (2007) where swine arteries were used and Misra and Singh (1983) who modeled perivascular tissue as linearly elastic material. Impossibility to measure perivascular pressure directly suggests that modeling PVAT as a real body could be more reliable approach.

One obvious barrier to considering PVAT in computational simulations as a 3D object is the fact that such an object has to be characterized with a constitutive equation to mathematically express its mechanical behavior. However, current scientific literature describing the elastic properties of PVAT at finite strains is very poor. In fact, we have not found any experimental study involving perivascular adipose tissue from human donors where mechanical tests aimed at describing the nonlinear elastic properties of PVAT at large strains has been carried out. It is worth noting that this finding is the main source of motivation for present study.

The many experiments available in the literature have been conducted with subcutaneous adipose tissue, usually from the abdominal region or from the breast, because their primary goal was to provide data suitable for computational simulations focused on plastic and reconstructive surgery (Sommer et al., 2013; Omidi et al., 2014). Moreover, most of these studies adopted the linear model and describe the elasticity of adipose tissue by means of the Young modulus (Geerligs et al., 2008; Comley and Fleck, 2010). The framework of nonlinear elasticity was adopted by Sommer et al. (2013), Omidi et al. (2014), and Calvo-Galleo et al. (2018), but they did not focus on perivascular tissue.

2. Aim of the Study

It is clear from above mentioned that the abdominal aorta is a prominent site where various diseases can develop. They can change blood flow in the aorta substantially or even can threaten patient's life due to purely mechanical events like aneurysm rupture. Thus from biomechanical point of view, the abdominal aorta still needs scientific attention. Particularly, its boundary conditions – perivascular tissue-aorta force interaction and axial prestretch – seem to be scientifically undervalued. This thesis is written with an aim to contribute to fill this gap. Its objectives are as follow.

This work aims to confirm the significant influence of boundary conditions on the mechanical condition of the abdominal aorta. To confirm this hypothesis was considered:

1. mechanical interaction of the abdominal aorta with human perivascular adipose tissue on its outer radius in order to obtain that it is necessary

- to identify mechanical properties by perform experiments with human perivascular adipose tissue,
- to identify constitutive model of perivascular adipose tissue and then it is necessary to create analytical model by simulation of inflation-extension test of bilayer tube (abdominal aorta surrounded by perivascular adopise tissue).

2. application of axial prestretch on ends of the abdominal aorta which is surrounding by perivascular adipose tissue in order to achieve investigation under realistic conditions.

3. Materials and Methods

3.1 Tensile testing of adipose tissue

Samples. Specimens were obtained from cadavers autopsied in the Department of Forensic Medicine of Královské Vinohrady University Hospital in Prague. The post-mortem usage of human tissue was approved by the Ethics Committee of the Third Faculty of Medicine of Charles University in Prague. Figure 3 shows the aorta surrounded by adipose tissue. Approximately rectangular strips with typical dimensions of 10 mm x 10 mm x 50 mm were prepared using a scalpel. The reference dimensions of the samples were determined by image analysis of digital photographs (NIS-Elements, Nikon Instruments). Due to high compliance and the slipperiness of the tissue, it was not possible to perfectly align the strips in either circumferential or longitudinal directions [Voňavková and Horný, 2020; Vonavkova et al., 2015; Voňavková et al., 2014].

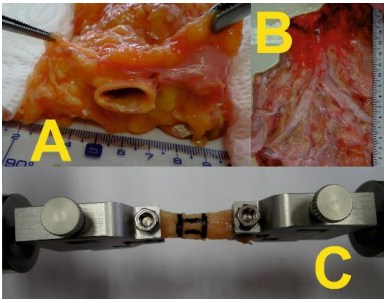

Figure 3. Perivascular tissue surrounds infrarenal aorta – transversal plane (panel A), frontal plane (panel B). A sample of PVAT in uniaxial tension (panel C). Adopted from [Voňavková and Horný, 2020; Vonavkova et al., 2015; Voňavková et al., 2014].

Testing procedure. A multipurpose tensile testing machine (Zwick/Roell, Germany) was used. The testing machine used electromechanical actuators with a displacement resolution of ± 1 μm and U9B force transducers (HBM, Germany, ± 25 N). During the test, the deformation of samples was

determined with a built-in videoextensometer by means of contrasting marks created on a sample with liquid eyeliner. The experimental protocol consisted of four cycles as a preconditioning of tissue behavior, and the fifth cycle was used in the subsequent determination of the material parameters. The loading part of the force–elongation response was used for this purpose. All tests were conducted at room temperature with the velocity of clamps set to 0.2 mms^{-1} [Voňavková and Horný, 2020; Vonavkova et al., 2015; Voňavková et al., 2014].

3.2 PVAT constitutive model and its parameters

Kinematics. It was assumed that during the uniaxial tensile test, the portion of the sample restricted by marks undergoes homogenous dilatation expressed in Cartesian coordinates as $x_i = \lambda_{iK} X_K$ for i, K = 1, 2, and 3 where $\lambda_{iK} = 0$ for $i \neq K$. Here $\boldsymbol{X} = (X_1, X_2, X_3)^T$ and $\boldsymbol{x} = (x_1, x_2, x_3)^T$ respectively denote the position vector in the reference and in the deformed configuration. Deformation gradient **F** is defined in (1) and the right Cauchy-Green strain tensor **C** is given by $\mathbf{C} = \mathbf{F}^T\mathbf{F}$ [Voňavková and Horný, 2020; Vonavkova et al., 2015; Voňavková et al., 2014].

$$\mathbf{F} = \frac{\partial \boldsymbol{x}}{\partial \boldsymbol{X}} \tag{1}$$

Due to high lipid content in the adipose tissue, it is assumed that PVAT is incompressible (Comley and Fleck, 2010; Sommer et al., 2013), thus $det(\mathbf{F}) = 1$ holds during the deformation.

Constitutive model. Since our aim was to use data characterizing PVAT in time-independent (quasi-static) simulations of the inflation-extension behavior of the abdominal aorta, we restricted our attention to the elastic response of PVAT. It means that viscoelastic effects, like stress relaxation and creep, which may accompany in vivo pressure wave propagation, are

neglected here. Thus perivascular adipose tissue was considered to be hyperelastic (Sommer et al., 2013; Omidi et al., 2014). It was characterized with the strain energy density function expressed in (2). Here c_1, and c_2 denote stress-like material parameters, and I_1 is the first invariant of the right Cauchy-Green deformation tensor **C**. The isotropic elastic potential (2) was chosen in accordance with Omidi et al. (2014). An assumption of isotropy was adopted because we were not able to perfectly align samples with anatomical directions [Voňavková and Horný, 2020].

$$W_{PT} = c_1\left(I_1 - 3\right) + c_2\left(I_1 - 3\right)^2 \tag{2}$$

The hyperelastic constitutive equation for incompressible material is given by (3). Here $\boldsymbol{\sigma}$ denotes the Cauchy stress tensor, and **I** is the second order unit tensor. The symbol p denotes the indeterminate multiplier related to the hydrostatic part of the stress tensor [Voňavková and Horný, 2020].

$$\boldsymbol{\sigma} = \frac{\partial W}{\partial \mathbf{F}}\mathbf{F}^T - p\mathbf{I} \tag{3}$$

Regression analysis. Experimental stress was obtained as $\sigma_{11}^{EXP} = F\lambda_{11}/S$, where S denotes the reference cross-section area and F is the force elongating the sample from reference length L to deformed length l; $\lambda_{11} = l/L$. The stress predicted by the model, σ_{11}^{MOD}, is obtained from (3), and its final expression is given in (4) [Voňavková and Horný, 2020].

$$\sigma_{11}^{MOD} = 2\left(c_1 + 2c_2\left(\lambda_{11}^2 + \frac{2}{\lambda_{11}} - 3\right)\right)\left(\lambda_{11}^2 - \frac{1}{\lambda_{11}}\right) \tag{4}$$

3.3 Constitutive model for abdominal aorta

The abdominal aorta wall was modeled as a homogenous, anisotropic, incompressible and hyperelastic continuum characterized by the strain energy

density function W_A proposed by Gasser et al. (2006). It is expressed in (5) [Voňavková and Horný, 2020; Vonavkova et al., 2016].

$$W_A = \frac{\mu}{2}\left(I_1 - 3\right) + \sum_{i=4,6} \frac{k_1}{2k_2}\left(e^{k_2\left(K_i - 1\right)^2} - 1\right) \tag{5}$$

$$K_i = \kappa I_1 + \left(1 - 3\kappa\right) I_i \qquad i = 4,6 \tag{6}$$

The elastic potential (5) consists of an isotropic part, it is a neo-Hookean term depending on the first invariant of **C**, and an anisotropic exponential part that depends on generalized structural deformation invariants denoted K_4 and K_6. The isotropic part is related to the elastic energy stored in the non-collagenous part of the arterial wall, whereas the anisotropic part is linked to the energy stored in bundles of collagen fibers. Since these fibers have a stochastic wavy pattern, their recruitment into the load-bearing process results in the strain-stiffening response, which is well described by an exponential function (Holzapfel et al., 2000). The model is based on the assumption that bundles of collagen fibers are arranged in the arterial wall with two dominant helices wound around the longitudinal axis at angles of ± (90° – β). These helices can be in cylindrical coordinates (R, Θ, Z) characterized with unit vectors $\boldsymbol{M}_1 = (0, cos\ (\beta), sin\ (\beta))^T$, $\boldsymbol{M}_2 = (0, cos\ (-\beta), sin\ (-\beta))^T$. These preferred directions give rise to deformation invariants I_4 and I_6 according to (7) [Voňavková and Horný, 2020; Vonavkova et al., 2016].

$$I_4 = \boldsymbol{M}_1 \cdot \left(\mathbf{C}\boldsymbol{M}_1\right) = \boldsymbol{M}_2 \cdot \left(\mathbf{C}\boldsymbol{M}_2\right) = I_6 \tag{7}$$

In fact, however, the collagen fibers are not perfectly aligned with the directions $\boldsymbol{M}_1$ and $\boldsymbol{M}_2$. Rather, they exhibit some dispersion around the predominant directions. The used strain energy function takes this into account by using generalized structural invariants K_4 and K_6 that also include a contribution from invariant I_1. Nevertheless, it is worth noting that although the model (5) enables structural interpretation, in fact it is phenomenological

model and its parameters should not be confused with exact internal architecture of arterial wall [Voňavková and Horný, 2020; Vonavkova et al., 2016].

3.4 Simulation of the inflation-extension behavior of the abdominal aorta with PVAT

Geometry and kinematics. The abdominal aorta was modeled as a homogenous thick-walled tube with the reference geometry corresponding to an open cylinder to take into account circumferential residual strains (Horný et al., 2014a,b). Hence in the first step, the reference stress-free opened cylinder is closed to form a hollow cylinder. The kinematics in polar cylindrical coordinates is expressed in equations (8). (ρ, ϑ, ζ) are coordinates defined in the stress-free configuration, whereas (R, Θ, Z) are defined in the residually stressed but unpressurized state. In equations (8b) and (8c), α is the opening angle, and δ is the axial stretch accompanying closing into cylindrical geometry [Voňavková and Horný, 2020; Vonavkova et al., 2016].

$$R = R(\rho) \qquad \Theta = 2\pi/(2\pi - 2\alpha)\vartheta \qquad Z = \delta\zeta \tag{8}$$

Subsequently, the aorta is elongated by axial force F_{red} to reach its in situ length, and inflation by internal pressure P follows. During pressurization, the aorta can further elongate or shorten, and that is governed by equilibrium equations. In (9), the deformed configuration is expressed in the polar cylindrical coordinates (r, θ, z) [Voňavková and Horný, 2020].

$$r = r(R) \qquad \theta = \Theta \qquad z = \lambda Z \tag{9}$$

The total deformation gradient of the aorta $\mathbf{F}_A$ is then given as $\mathbf{F}_A = \mathbf{F}_{A2}\mathbf{F}_{A1}$, where $\mathbf{F}_{A1}$ is linked to the residual deformation and $\mathbf{F}_{A2}$ expresses subsequent inflation and extension. The matrices of the gradients are given in (10) and (11) [Voňavková and Horný, 2020; Vonavkova et al., 2016].

$$\mathbf{F}_A = \mathbf{F}_2\mathbf{F}_1 = \begin{pmatrix} \lambda_{r\rho} & 0 & 0 \\ 0 & \lambda_{\vartheta\vartheta} & 0 \\ 0 & 0 & \lambda_{z\zeta} \end{pmatrix} = \begin{pmatrix} \partial r/\partial\rho & 0 & 0 \\ 0 & \pi r/\left[\rho(\pi-\alpha)\right] & 0 \\ 0 & 0 & \lambda\delta \end{pmatrix} \tag{10}$$

$$\mathbf{F}_{A1} = \begin{pmatrix} \lambda_{R\rho} & 0 & 0 \\ 0 & \lambda_{\Theta\vartheta} & 0 \\ 0 & 0 & \lambda_{Z\zeta} \end{pmatrix} = \begin{pmatrix} \partial R/\partial\rho & 0 & 0 \\ 0 & \pi R/\left[\rho(\pi-\alpha)\right] & 0 \\ 0 & 0 & \delta \end{pmatrix} \tag{11}$$

$$\mathbf{F}_{A2} = \begin{pmatrix} \lambda_{rR} & 0 & 0 \\ 0 & \lambda_{\vartheta\Theta} & 0 \\ 0 & 0 & \lambda_{zZ} \end{pmatrix} = \begin{pmatrix} \partial r/\partial R & 0 & 0 \\ 0 & r/R & 0 \\ 0 & 0 & \lambda \end{pmatrix} \tag{12}$$

To account for the effect of perivascular tissue on the mechanics of the aorta, it is assumed that during its inflation and extension the aorta is surrounded by an external cylindrical layer composed of PVAT. $R_{oA} = R_{iPT}$ and $r_{oA} = r_{iPT}$ hold during the deformation. Here R_{iPT} and r_{iPT} denote the reference and deformed inner radius of the PVAT cylinder, Figure 4. It is assumed that the PVAT cylinder retains its cylindrical shape in the deformation, thus its deformation gradient has a form similar to $\mathbf{F}_{A2}$ [Voňavková and Horný, 2020; Vonavkova et al., 2016].

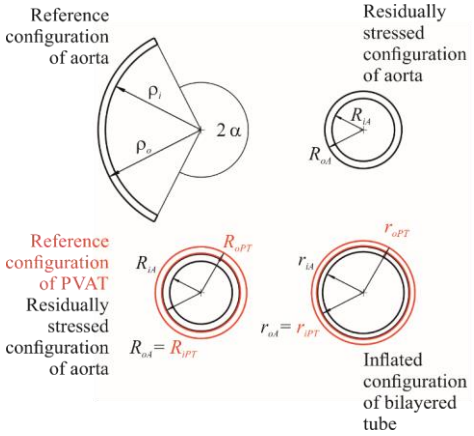

Figure 4. Reference and deformed configurations. Adopted from [Voňavková and Horný, 2020].

Equilibrium equations. Equilibrium equations for the bi-layered tube can be written in the forms (13-14). Here $\hat{W}$ denotes W with radial stretch being substituted from the incompressibility condition. W_A represents the strain energy stored in the aorta (5), and W_{PT} denotes the energy stored in PVAT (2) [Voňavková and Horný, 2020; Vonavkova et al., 2016].

$$P = \int_{r_{iA}}^{r_{oA}} \lambda_{\vartheta\vartheta} \frac{\partial \hat{W}_A}{\partial \lambda_{\vartheta\vartheta}} \frac{dr}{r} + \int_{r_{iPT}}^{r_{oPT}} \lambda_{\Theta\Theta} \frac{\partial \hat{W}_{PT}}{\partial \lambda_{\Theta\Theta}} \frac{dr}{r} \tag{13}$$

$$F_{red} = \pi \int_{r_{iA}}^{r_{oA}} \left(2\lambda_{z\zeta} \frac{\partial \hat{W}_A}{\partial \lambda_{z\zeta}} - \lambda_{\vartheta\vartheta} \frac{\partial \hat{W}_A}{\partial \lambda_{\vartheta\vartheta}} \right) r dr + \pi \int_{r_{iPT}}^{r_{oPT}} \left(2\lambda_{zZ} \frac{\partial \hat{W}_{PT}}{\partial \lambda_{zZ}} - \lambda_{\Theta\Theta} \frac{\partial \hat{W}_{PT}}{\partial \lambda_{\Theta\Theta}} \right) r dr \tag{14}$$

Equations (13) and (14) assume that the boundary conditions $\sigma_{rr}(r_{iA}) = -P \wedge \sigma_{rr}(r_{oPT}) = 0$ hold. The tube is considered to be closed, and F_{red} is an additional axial force which ensures the initial axial stretch ($\lambda_{z\zeta}^{ini}$) and which the aorta sustains independently of internal pressure P (Horný et al., 2013, 2014b, 2017).

3.5 Stress distribution through the wall

To evaluate stress distribution through the wall, equations (15a), (15b), and (15c) have been adopted. Stresses acting in PVAT are obtained when substitution from (2) is performed, and $\lambda_{\Theta\Theta}$, λ_{zZ}, and integration to r_{oPT} is considered [Voňavková and Horný, 2020; Vonavkova et al., 2016].

$$\sigma_{rr}(r) = -\int_{r}^{r_{oA}} \lambda_{\vartheta\vartheta} \frac{\partial \hat{W}_A}{\partial \lambda_{\vartheta\vartheta}} \frac{dx}{x} - \int_{r_{iPT}}^{r_{oPT}} \lambda_{\Theta\Theta} \frac{\partial \hat{W}_{PT}}{\partial \lambda_{\Theta\Theta}} \frac{dr}{r}$$

$$\sigma_{\theta\theta}(r) = \lambda_{\vartheta\vartheta} \frac{\partial \hat{W}_A}{\partial \lambda_{\vartheta\vartheta}} + \sigma_{rr}$$

$$\sigma_{zz}(r) = \lambda_{z\zeta} \frac{\partial \hat{W}_A}{\partial \lambda_{z\zeta}} + \sigma_{rr} \tag{15}$$

3.6 Thickness of PVAT, loading conditions and material parameters

PVAT thickness. With regard to amount of fat tissue, anatomical variations in human population are rather large. To take this fact into account, three representative thicknesses of the PVAT layer were considered in our simulations. These cases were chosen with reference to the thickness of the aorta such that: (I) represents very thin fat layer with 0.2 mm = $H_{PT} \ll R_{oA} - R_{iA}$, (II) $H_{PT} = R_{oA} - R_{iA}$ is middle case, and (III) $R_{oA} - R_{iA} \ll H_{PT}$ = 40 mm represents a situation that the movement of aorta is significantly restricted with surrounding tissue [Voňavková and Horný, 2020].

Loading. External loading during the inflation-extension response of the aorta is represented by internal pressure P and the initial axial stretch $\lambda_{z\zeta}^{ini}$ that the aorta sustains independently of pressure. To account for prestretch, F_{red} necessary to elongate the aorta to $\lambda_{z\zeta}^{ini}$ was computed at P = 0. In the subsequent pressurization from 0 up to 16 kPa, F_{red} was held constant, which ensured that $\lambda_{z\zeta}$ would vary during inflation. Values where $\lambda_{z\zeta}^{ini}$ = 1, 1.1, and 1.2 were considered in our study [Voňavková and Horný, 2020].

Material parameters for aorta and PVAT. The material parameters for the abdominal aorta were adopted from Horný et al. (2014a). One representative sample of a 38 year old male donor was considered (denoted M38). The specific values of the material parameters are in Table 1. In contrast to aortic tissue, the PVAT parameters are based on our experiments. In the inflation-extension simulation, average perivascular tissue behavior was considered. Since the constitutive equation for PVAT is nonlinear, the material parameters used in the study were fitted to all the data to obtain a mean model. Such an approach takes into account the effects of all observed responses and naturally produces a model which can be considered an average model [Voňavková and Horný, 2020; Vonavkova et al., 2016].

Table 1. Constitutive parameters and geometry of the human abdominal aorta. Adopted from Horný et al. (2014a).

	Sex	Age [years]	μ [kPa]	k_1 [kPa]	k_2 [–]	κ [–]	β [°]	ρ_i [mm]	ρ_o [mm]	α [°]	R_{iA} [mm]	R_{oA} [mm]
M38	Male	38	15.9	78.49	4.99	0.19	41.41	16.2	17.24	117	5.3	6.52

4. Results and Discussion

4.1 Constitutive behavior of adipose tissue

Fifteen successful uniaxial tensile tests were conducted with samples of PVAT obtained from seven donors. Table 2 summarizes the age, sex, and number of samples obtained from each donor. The samples exhibited a nonlinear response at large strains, Figure 5. The model curves were computed by means of least square optimization for: (a) the most compliant case, (b) with all measured data pooled together which resulted in the set of material parameters that represents the average mechanical behavior, and finally (c) the stiffest case. The estimated material parameters appear in Table 2 [Voňavková and Horný, 2020].

Table 2. PVAT samples summary and material parameters (a – the most compliant case, b – average model, c – the stiffest case). Adopted from [Voňavková and Horný, 2020].

Donor	Sex {M,}	Age [years]	n [–]
1	M	71	3
2	M	41	3
3	M	67	2
4	M	71	1
5	F	53	1
6	M	29	3
7	M	69	2

	c_1 [kPa]	c_2 [kPa]
(a)	0.1	89.7
(b)	0.723	418
(c)	5.46	1439

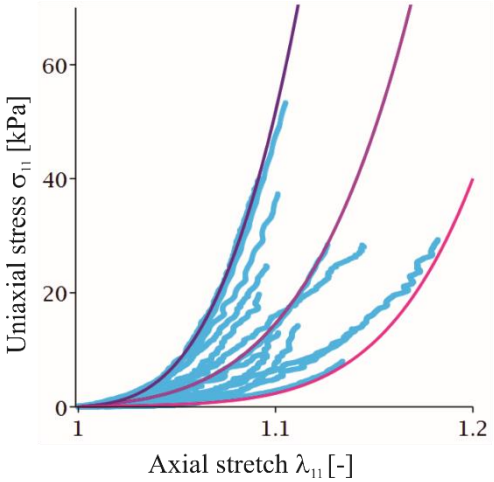

Figure 5. Uniaxial tensile tests of PVAT and model curves.
Adopted from [Voňavková and Horný, 2020].

The uniaxial tensile tests confirmed that the elastic response of PVAT, similar to subcutaneous fatty tissue, is highly nonlinear (Sommer et al., 2013; Calvo-Gallego et al., 2018). Unfortunately, in contrast to Sommer et al. (2013), we cannot conclude that the observed behavior suggests anisotropic material properties, because we were not able to ensure the constant orientation of the samples during their separation. The highly compliant response of the tissue complicated manual preparation.

Omidi et al. (2014) studied the mechanical behavior of adipose tissue in subcutaneous abdominal region by means of an indentation test. They employed the Yeoh hyperelastic model (third order polynomial in I_1) to express the constitutive properties of the tissue. They arrived at values of the material parameters that seems to be somewhat lower than found in our study. c_1 = 0.16 kPa, c_2 = 0.018 kPa, and $c_3 = 1.1 \cdot 10^{-7}$ kPa are typical values estimated by Omidi et al. (2014). This discrepancy may be partially attributed to a different experimental technique used in Omidi et al. (2014), but the

most important difference seems to be the fact that Omidi et al. (2014) decellularized the tissue before testing, which can significantly change the mechanical properties of tissues (Bielli et al., 2018; Liao et al., 2008).

Although adipose tissue is very compliant and small values of an acting force can deform such an object to a state which requires employing the finite strain theory, small strain approximations are sometimes used in the literature. In this approach, the framework of linear elasticity is appropriate, and one can find studies reporting values for the Young elastic modulus for adipose tissue. Restricting our attention to the small strain theory, we can substitute the nonlinear model (2) with the slope of the tangent computed to a stress–strain curve at the beginning of the deformation. This slope is referred to as the initial elastic modulus. A consideration of the material parameters presented in Table 2 leads to 0.6 kPa, for the most compliant material response, to 4.3 kPa for average response, and to 32.7 kPa for the stiffest case. Omidi et al. (2014) reported 3.4 kPa for the Young modulus obtained for abdominal subcutaneous tissue. Comley and Fleck (2010, 2012), Nightingale et al. (2003), and Miller-Young et al. (2002) reported a Young modulus in the range of 1 – 14 kPa depending on the source of the tissue and applied strain rate. Geerligs et al. (2008) reported the shear elastic modulus of subcutaneous tissue to be of 7.5 kPa that implies a elastic modulus of about 22 kPa. Thus, we conclude that our data suggest somewhat stiffer behavior for perivascular adipose tissue than is known for subcutaneous tissue; however, under small strains they do not differ significantly.

4.2 Inflation-extension response of abdominal aorta surrounded with adipose tissue

The effect of perivascular adipose tissue on the mechanics of the abdominal aorta was simulated by means of an analytical model based on the bi-layered thick-walled tube problem formulated within a framework of nonlinear elasticity and numerically solved in Maple. Figures 8 and 9 show the

resulting inflation and extension behavior in terms of deformed radius and axial stretch obtained for the 38-year-old male individual (M38). To highlight the effect of PVAT and axial prestretch on the circumferential response of the aorta, Figure 8 depicts the dependence between circumferential stretch (computed at r_{iA}) and the inflating pressure. Figures 11 (aorta) and 12 (PVAT) show the stress distribution through the thickness of the wall computed at loading pressure P = 16 kPa for tubes with different H_{PT} and $\lambda_{z\zeta}^{ini}$ [Voňavková and Horný, 2020].

With regard to inflation behavior, the figures document that PVAT restricts the radial motion of an artery. It is exhibited in each studied position (r_{iA}, $r_{oA} = r_{iPT}$, and r_{oPT}; see Figure 6). Where r_{oPT} for H_{PT} = 40 mm, the movement is almost negligible in comparison with the thickness of the fatty tissue. Thus, one could hypothetically conclude that the presence of the fatty surrounding is mechanically disadvantageous for the human body, because it prevents an artery from functioning as an elastic capacitor in the Windkessel effect. Later, we will see that this is just one side of the coin.

In contrast to PVAT, axial prestretch has, in the range of physiological pressure, the absolutely opposite effect. Figure 6 document that the $P - r$ responses are more compliant when longitudinal pretension is applied. Perhaps it is most clearly depicted in Figure 8, where circumferential stretch at the inner radius of the aorta is presented. In accordance with our previous study, Horný et al. (2014b), it can be said that the axial prestrain of the tube leads to higher circumferential distensibility in the inflation carried out at physiological pressures. Since the distensibility may not be easily recognized from the figure, Table 3 includes the specific results obtained for H_{PT} and $\lambda_{z\zeta}^{ini}$. The distensibility is quantified as (r_{iA}(16kPa) – r_{iA}(10kPa))/r_{iA}(10kPa). From Table 3, we can conclude that, although increasing H_{PT} leads to decreasing distensibility, axial preloading balances this influence [Voňavková and Horný, 2020].

Table 3. Specific values of distensibility, $(r_{iA}(16\text{kPa}) - r_{iA}(10\text{kPa}))/r_{iA}(10\text{kPa})$, obtained from the curves in Figure 8. Adopted from [Voňavková and Horný, 2020].

	M38	H_{PT} = 0.2 mm	$H_{PT} = H_A$	H_{PT} = 40 mm
$\lambda_{z\zeta}^{ini} = 1$		0.0469	0.0333	0.0279
$\lambda_{z\zeta}^{ini} = 1.1$		0.0521	0.0340	0.0390
$\lambda_{z\zeta}^{ini} = 1.2$		0.0631	0.0612	0.0454

The axial response is depicted in Figure 7. We again observe that including perivascular tissue into the model has, similar to circumferential behavior, an immobilization effect. The dark curves corresponding to H_{PT} = 40 mm exhibit a lower stretch variation, $\lambda_{z\zeta}(P_2) - \lambda_{z\zeta}(P_1)$ for $P_1 < P_2$, than the light curves obtained for the thinner PVAT layers. At typical physiological pressures, P_2 = 16 kPa and P_1 = 10 kPa, it is also visible for $\lambda_{z\zeta}^{ini}$ = 1.1. In this case, the curve corresponding to H_{PT} = 40 mm is almost perpendicular to the horizontal axis of the graph, which suggests that the prestretched tube does not move axially during the pressure pulse [Voňavková and Horný, 2020]. It has been hypothesized in the literature that minimization of the axial movement during the pressure pulse transmission is advantageous for arteries (Schulze-Bauer et al., 2003). Our results show that PVAT contributes to the minimization of axial movement of the aorta.

On the other hand, comparing the panels created for $\lambda_{z\zeta}^{ini}$ = 1.2 with panels for $\lambda_{z\zeta}^{ini}$ = 1.1 indicates that this behavior is not monotonic. It does not hold true in the sense that the higher the prestretch the lower the axial movement would generally be. Where $\lambda_{z\zeta}^{ini}$ = 1.2, the lowest variation of axial deformation is obtained for H_{PT} = 0.2 mm. However, human arteries are not prestrained without limits. For the abdominal aorta, typical values can be found in Horný et al. (2014b, 2017). These studies suggest $\lambda_{z\zeta}^{ini}$ = 1.179 for M38 is to be expected. The value come from the studied interval $\lambda_{z\zeta}^{ini}$ = 1 – 1.2. Computations show that somewhere inside this interval the longitudinal

response changes from pressure-induced elongation to pressure-induced shortening. Our results suggest that the expected values of prestretch, presented in Horný et al. (2014b), fall close to a hypothetical optimal point not only in the case of bare aortas but also when the existence of PVAT and its mechanical role are considered [Voňavková and Horný, 2020].

In accordance with a solution known from the classical theory of elasticity for the bi-layered thick-walled tube, the computed distribution of radial stress confirms that PVAT bears some portion of the pressure load. Transmural pressure loading PVAT, $-\Delta P_{PT} = \sigma_{rr}(r_{iPT}) - \sigma_{rr}(r_{oPT}) = \sigma_{rr}(r_{iPT})$, increases when the thickness of PVAT increases. Reciprocally, the thicker the PVAT layer is, the lower is the loading of the aorta, $-\Delta P_A = \sigma_{rr}(r_{iA}) - \sigma_{rr}(r_{oA}) = -P + \Delta P_{PT}$. As a consequence of the decreasing loading of the aorta, the increasing thickness of PVAT causes a decrease in circumferential and axial stresses. This is another example showing that the existence of PVAT is advantageous from a mechanical point of view. It bears some portion of the loading and thus decreases the load acting on the aorta itself.

The role of axial prestretch is very interesting. The middle row in Figure 9 show that increasing axial pretension leads to a decrease in circumferential stress in the aorta. Where $\lambda_{z\zeta}^{jni} = 1.2$ and $H_{PT} = 40$ mm, negative values for $\sigma_{\theta\theta}$ at r_{iA} are even reached. Interestingly, in the PVAT layer, an increase in circumferential stress at r_{iPT} is observed for $H_{PT} = 0.2$ (Figure 10). However, the maximum value of circumferential stress decreases with increasing $\lambda_{z\zeta}^{jni}$ for $H_{PT} = H_A$ and $H_{PT} = 40$ mm. This documents that the effect of axial pretension is not monotonic with respect to the simultaneous effect of the thickness [Voňavková and Horný, 2020].

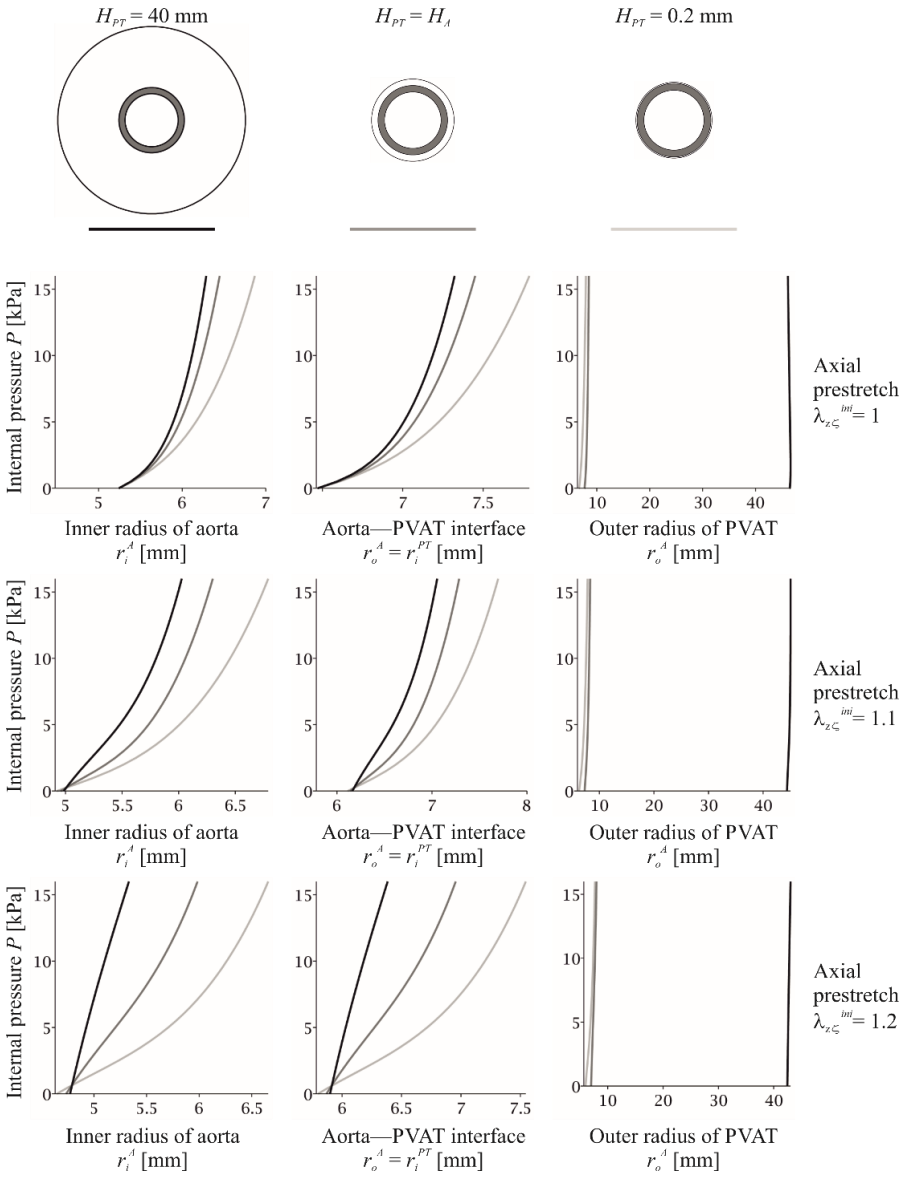

Figure 6. Inflation response of abdominal aorta M38 surrounded by PVAT with H_{PT} = 0.2, 1.22, and 40 mm.
Adopted from [Voňavková and Horný, 2020].

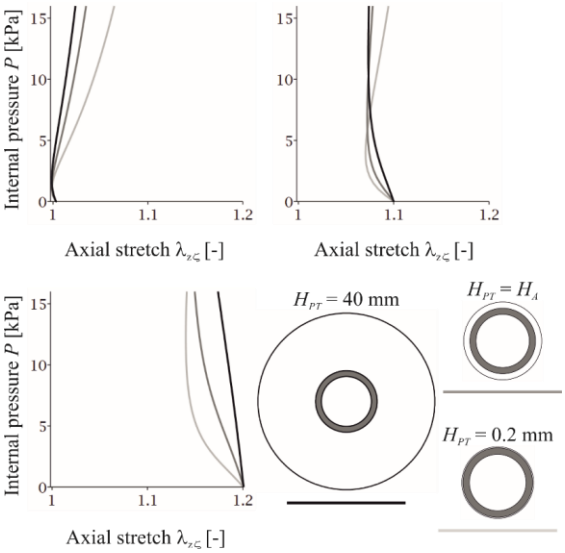

Figure 7. Extension response of abdominal aorta M38 surrounded by PVAT with H_{PT} = 0.2, 1.22, and 40 mm. Adopted from [Voňavková and Horný, 2020].

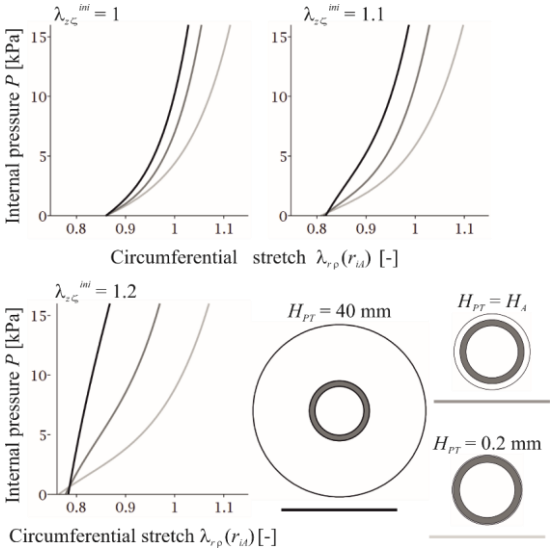

Figure 8. Dependence of circumferential stretch at the inner radius of the aorta during inflation of M38 on axial prestretch. Adopted from [Voňavková and Horný, 2020].

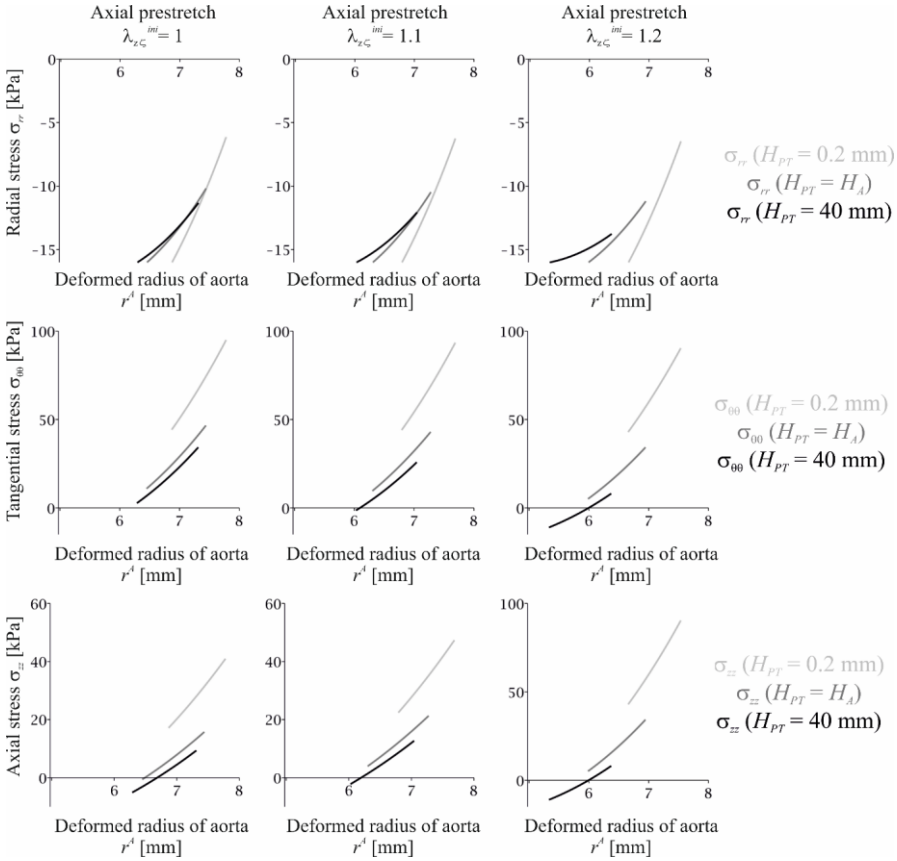

Figure 9. Distribution of in-wall stresses in aorta M38 pressurized to 16 kPa and surrounded by PVAT with H_{PT} = 0.2, 1.22, and 40 mm.
Adopted from [Voňavková and Horný, 2020].

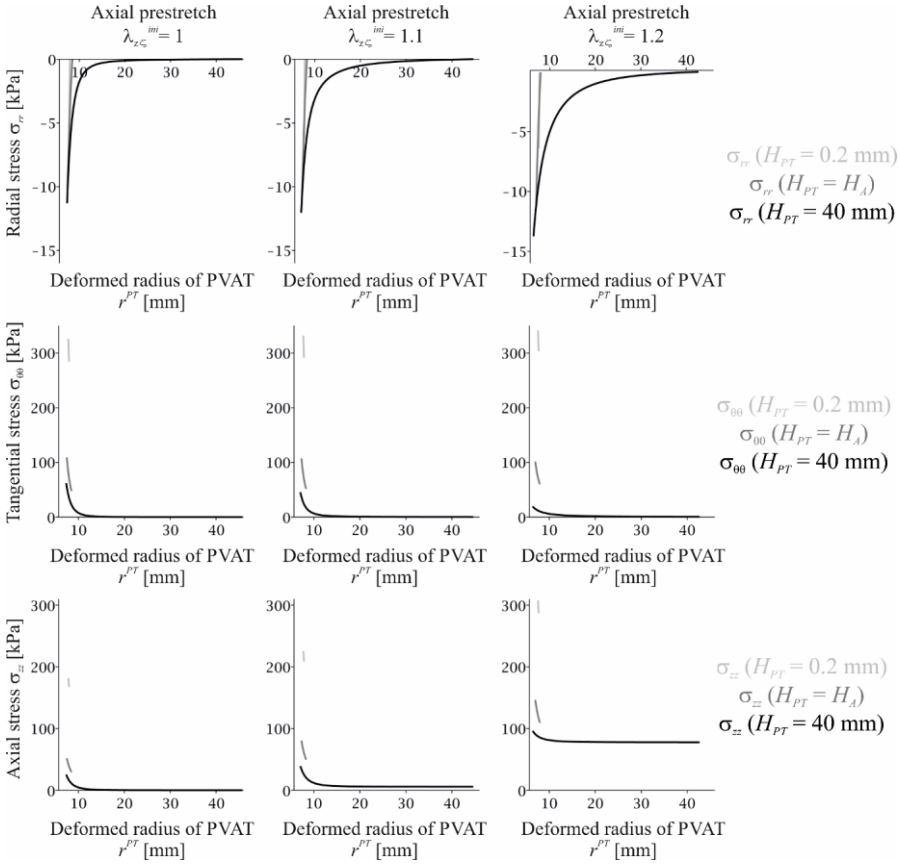

Figure 10. Distribution of in-wall stresses in PVAT at P = 16 kPa. PVAT tube thickness was H_{PT} = 0.2, 1.22, and 40 mm.
Adopted from [Voňavková and Horný, 2020].

5. Conclusion

Constitutive parameters of perivascular adipose tissue were found in our study. A hyperelastic constitutive description was employed in the form of the Yeoh strain energy density. The obtained material parameters were subsequently used in the analytical solution of the bi-layer thick-walled tube problem simulating the mechanical effect of PVAT on the abdominal aorta. Simultaneous with examining the effect of PVAT, the effect of axial prestretch was also studied. It was found that the presence of PVAT reduces the distensibility. Axial prestretch applied to the aorta embedded in PVAT had an opposite effect. Axially prestrained aortas exhibited higher distensiblity than non-prestrained aortas. It was also shown that the perivascular envelope bears some portion of the pressure loading and thus reduces the mechanical stresses inside the wall of the aorta. A similar effect was found for axial prestretch. The results suggest that perivascular adipose tissue is mechanically advantageous, due to it reducing wall stresses, and that decreased arterial distensibilty is compensated for by axial prestretch in the aorta.

List of author´s publications

Publications on topic of the dissertation thesis

Voňavková and Horný (2020) Effect of axial prestretch and adipose tissue on the inflation-extension behavior of the human abdominal aorta. Computer Methods in Biomechanics and Biomedical Engineering 23(3):81-91.

Publisher link: https://doi.org/10.1080/10255842.2019.1699544. Article in journal with WoS impact factor (IF2018 = 1.61).

Vonavkova, T., Horny, L., Vesely, J., Adamek, T., and Zitny, R. (2016) Effect of perivascular tissue on inflation-extension behavior of abdominal aorta. ECCOMAS Congress 2016: VII European Congress on Computational Methods in Applied Sciences and Engineering. p. 6616-6624.

Publisher link: https://doi.org/10.7712/100016.2283.10742. Conference paper indexed in SCOPUS/WoS.

Vonavkova, T., Horny, L., Adamek, T., Kulvajtova, M.,Zitny, R. (2015) Constitutive modelling of human perivascular adipose tissue. A: COMPLAS XIII. "COMPLAS XIII: proceedings of the XIII International Conference on Computational Plasticity: fundamentals and applications". CIMNE ed. Barcelona: CIMNE, p. 463-470.

Conference paper indexed in SCOPUS/WoS.

Voňavková T., Horný L., Kulvajtová M., Žitný R. (2014). Uniaxial tensile test of perivascular adipose tissue. *Bulletin of Applied Mechanics* 10(36):11-14. ISSN 1801-1217.

Article in peer-reviewed journal.

Other publications

Suchý T., Šupová M., Klapková E., Adámková V., Závora J., Žaloudková M., Rýglová Š., Ballay R., Denk F., Pokorný M., Sauerová P., Hubálek Kalbáčová M., Horný L., Veselý J., Voňavková T., Průša R. (2017). The release kinetics, antimicrobial activity and cytocompatibility of differently prepared collagen/hydroxyapatite/vancomycin layers: Microstructure vs. Nanostructure. *Eur J Pharm Sci*, 100:219-229.

Publisher link: https://doi.org/10.1016/j.ejps.2017.01.032. Article in journal with WoS impact factor (IF2018 = 3.532).

Horny, L., Chlup, H., Zitny, R., Vonavkova, T., Vesely, J., & Lanzer, P. (2012). Ex vivo coronary stent implantation evaluated with digital image correlation. *Exp Mech* 52(9), 1555-1558.

Publisher link: https://doi.org/10.1007/s11340-012-9620-6. Article in journal with WoS impact factor (IF2018 = 2.256).

Horny, L., Netusil, M., Vonavkova, T. (2014). Axial prestretch and circumferential distensibility in biomechanics of abdominal aorta. *Biomech Model Mechanobiol* 13(4):783-799.

Publisher link: https://doi.org/10.1007/s10237-013-0534-8. Article in journal with WoS impact factor (IF2018 = 2.829).

Horny, L., Chlup, H., Vesely, J., Gultova, E., Kronek, J., Zitny, R., Vonavkova, T., Adamek, T., Lanzer, P., and Hromadka, D. (2011) In vitro Coronary Stent Implantation: Vessel Wall-Stent Interaction.
5th European Conference of the International Federation for Medical and Biological Engineering. IFMBE Proceedings, vol 37. Springer, Berlin, Heidelberg.

Publisher link: https://doi.org/10.1007/978-3-642-23508-5_207. Conference paper indexed in SCOPUS/WoS.

References

Bielli A, Bernardini R, Varvaras D, Rossi P, Di Blasi G, Petrella G, Buonomo OC, Mattei M, Orlandi A. Characterization of a new decellularized bovine pericardial biological mesh: Structural and mechanical properties. J Mechan Behav Biomed Mater 2018;78:420-426.

Brown NK, Zhou Z, Zhang J, Zeng R, Wu J, Eitzman DT, Chen YE, Chang L. Perivascular adipose tissue in vascular function and disease: A review of current research and animal models. Arterioscler Thromb Vasc Biol 2014;34:1621-1630.

Calvo-Gallego JL, Domínguez J, Gómez Cía T, Gómez Ciriza G, Martínez-Reina J. Comparison of different constitutive models to characterize the viscoelastic properties of human abdominal adipose tissue. A pilot study. J Mechan Behav Biomed Mater 2018;80:293-302.

Comley K, Fleck NA. A micromechanical model for the young's modulus of adipose tissue. Int J Solids Struct 2010;47:2982-2990.

Comley K, Fleck N. The compressive response of porcine adipose tissue from low to high strain rate. Int J Impact Eng 2012;46:1-10.

Fereidoonnezhad, B., Naghdabadi, R., Sohrabpour, S., & Holzapfel, G. A. A mechanobiological model for damage-induced growth in arterial tissue with application to in-stent restenosis. Journal of the Mechanics and Physics of Solids 2017; 101; 311-327.

Gasser TC, Ogden RW, Holzapfel, GA. Hyperelastic modelling of arterial layers with distributed collagen fibre orientations. J Royal Soc Interface 2006;3:15-35.

Geerligs M, Peters GWM, Ackermans PAJ, Oomens CWJ, Baaijens FPT. Linear viscoelastic behavior of subcutaneous adipose tissue. Biorheology 2008;45:677-688.

Hejčl, A., Švihlová, H., Sejkorová, A., Radovnický, T., Adámek, D., Hron, J., Dragomir-Daescu, D., Málek, J., Sameš, M. (2017). Computational fluid dynamics of a fatal ruptured anterior communicating artery aneurysm. Journal of Neurological Surgery, Part A: Central European Neurosurgery, 78(6), 610-616. doi:10.1055/s-0037-1604286.

Hodis, S., & Zamir, M. (2009). Mechanical events within the arterial wall: The dynamic context for elastin fatigue. Journal of Biomechanics, 42(8), 1010-1016. doi:10.1016/j.jbiomech.2009.02.010.

Hodis S, Zamir M. Mechanical events within the arterial wall under the forces of pulsatile flow: A review. J Mechan Behav Biomed Mater 2011;4:1595-1602.

Holzapfel, G. A., Stadler, M., & Gasser, T. C. Changes in the mechanical environment of stenotic arteries during interaction with stents: Computational assessment of parametric stent designs. Journal of Biomechanical Engineering 2005; 127(1), 166-180.

Horny L, Adamek T, Zitny R. Age-related changes in longitudinal prestress in human abdominal aorta. Arch Appl Mech 2013;83:875-888.

Horný L, Netušil M, Daniel M. Limiting extensibility constitutive model with distributed fibre orientations and ageing of abdominal aorta. J Mechan Behav Biomed Mater 2014;38:39-51.

Horný L, Netušil M, Voňavková T. Axial prestretch and circumferential distensibility in biomechanics of abdominal aorta. Biomech Model Mechanobiol 2014;13:783-799.

Horný L, Adámek T, Kulvajtová M. A comparison of age-related changes in axial prestretch in human carotid arteries and in human abdominal aorta. Biomech Model Mechanobiol 2017;16:375-383.

Huang Cao, Z. F., Stoffel, E., & Cohen, P. Role of perivascular adipose tissue in vascular physiology and pathology. Hypertension 2017;69(5), 770-777.

Humphrey JD, Na S. Elastodynamics and arterial wall stress. Ann Biomed Eng 2002;30:509-523.

Kiousis, D. E., Gasser, T. C., & Holzapfel, G. A. A numerical model to study the interaction of vascular stents with human atherosclerotic lesions. Annals of Biomedical Engineering 2007; 35(11), 1857-1869.

Králová Lesná, I., Tonar, Z., Malek, I., Maluskova, J., Nedorost, L., Pirk, J., Pitha, J., Lanska, V., Poledne, R. Is the amount of coronary perivascular fat related to atherosclerosis? Physiological Research 2015;, 64, S435-S443.

Liao J, Joyce EM, Sacks MS. Effects of decellularization on the mechanical and structural properties of the porcine aortic valve leaflet. Biomaterials 2008;29:1065-1074.

Liu Y, Dang C, Garcia M, Gregersen H, Kassab GS. Surrounding tissues affect the passive mechanics of the vessel wall: Theory and experiment. Am J Physiol - Heart Circ Physiol 2007;293:H3290-H3300.

Masson I, Beaussier H, Boutouyrie P, Laurent S, Humphrey JD, Zidi M. Carotid artery mechanical properties and stresses quantified using in vivo data from normotensive and hypertensive humans. Biomech Model Mechanobiol 2011;10:867-882.

Miller-Young JE, Duncan NA, Baroud G. Material properties of the human calcaneal fat pad in compression: Experiment and theory. J Biomech 2002;35:1523-1531.

Moireau P, Xiao N, Astorino M, Figueroa CA, Chapelle D, Taylor CA, Gerbeau J. External tissue support and fluid-structure simulation in blood flows. Biomech Model Mechanobiol 2012;11:1-18.

Nightingale K, McAleavey S, Trahey G. Shear-wave generation using acoustic radiation force: In vivo and ex vivo results. Ultrasound Med Biol 2003;29:1715-1723.

Omidi E, Fuetterer L, Reza Mousavi S, Armstrong RC, Flynn LE, Samani A. Characterization and assessment of hyperelastic and elastic properties of decellularized human adipose tissues. J Biomech 2014;47:3657-3663.

Polzer, S., & Gasser, T. C. (2015). Biomechanical rupture risk assessment of abdominal aortic aneurysms based on a novel probabilistic rupture risk index. Journal of the Royal Society Interface, 12(113) doi:10.1098/rsif.2015.0852.

Schulze-Bauer CAJ, Mörth C, Holzapfel GA. Passive biaxial mechanical response of aged human iliac arteries. J Biomech Eng 2003;125:395-406. https://doi.org/10.1115/1.1574331.

Sommer G, Eder M, Kovacs L, Pathak H, Bonitz L, Mueller C, Regitnig P, Holzapfel GA. Multiaxial mechanical properties and constitutive modeling of human adipose tissue: A basis for preoperative simulations in plastic and reconstructive surgery. Acta Biomater 2013;9:9036-9048.

Zaborska KE, Wareing M, Austin C. Comparisons between perivascular adipose tissue and the endothelium in their modulation of vascular tone. B J Pharmacol 2017;174:3388-3397.

Zhang, W., Herrera, C., Atluri, S. N., & Kassab, G. S. (2004). Effect of surrounding tissue on vessel fluid and solid mechanics. Journal of Biomechanical Engineering, 126(6), 760-769. doi:10.1115/1.1824128.

Anotace

Cílem této dizertační práce je ukázat, že perivaskulární tuková tkáň může významně měnit mechanický stav břišní aorty. Za tímto účelem byly provedeny jednoosé tahové testy s perivaskulární tukovou tkání. V následné regresní analýze byly napěťově-deformační křivky nafitovány pomocí polynomické hustoty deformační energie. Konstitutivní model perivaskulární tukové tkáně byl použit v analytické simulaci chování inflace-extenze lidské abdominální aorty. Výpočetní model byl založen na teorii dvouvrstvé silnostěnné válcové trubice. Kromě účinku perivaskulární tkáně byl také studován vliv axiálního předpětí. Bylo zjištěno, že přítomnost perivaskulární tkáně snižuje roztažnost aorty. Axiální předpětí, aplikované na břišní aortu zabudovanou v tukové tkáni, mělo opačný účinek než účinek tukové tkáně. Axiálně předepjaté aorty vykazovaly vyšší roztažnost než nepředepjaté aorty. Dále bylo ukázáno, že perivaskulární obal nese určitou část tlakového zatížení a tím snižuje mechanické napětí uvnitř stěny břišní aorty. Podobný účinek byl nalezen pro axiální předpětí.

Summary

The dissertation thesis aims to show that perivascular adipose tissue may significantly change the mechanical state of the abdominal aorta. To this end, uniaxial tensile tests with perivascular fat tissue were carried out. In the subsequent regression analysis, stress-strain data were fitted by the polynomial strain energy density. A constitutive model of adipose tissue was used in the analytical simulation of the inflation-extension behavior of the human abdominal aorta. The computational model was based on the theory of the bi-layered thick-walled tube. In addition to the effect of perivascular tissue, the effect of axial prestretch was also studied. It was found that the presence of perivascular tissue reduces the distensibility of the aorta. Axial prestretch applied to aortas embedded in adipose tissue had an effect opposite to that of adipose tissue. Axially prestrained aortas exhibited higher distensiblity than non-prestrained aortas. It was also shown that the perivascular envelope bears some portion of the pressure loading and thus reduces the mechanical stresses inside the wall of aorta. A similar effect was found for axial prestretch.